Enhanced Direct Instantaneous Torque Control of Switched Reluctance Machine with Phase Current Limitation

D. Shah*, M. Hilairet◇, *member, IEEE,*, I. Bahri*
*LGEP/SPEE Labs; CNRS UMR8507; SUPELEC; Univ Pierre et Marie Curie-P6; Univ Paris Sud-P11, 91192 Gif sur Yvette, France
◇FEMTO-ST, CNRS UMR 6174, University of Franche-Comte, F-90010 Belfort, France
Email: mickael.hilairet@univ-fcomte.fr

***Abstract*—In this work, an Enhanced Direct Instantaneous Torque Control (EDITC)of a Switched Reluctance Machine is explored. The main issue of regular direct instantaneous torque control (DITC) is that the current is measured but not controlled. Therefore, a new algorithm for hysteresis-controller was provided which included additional feature such as current limiter. Several simulations are presented which validates our controller over wide range of speed and torque.**

***Index Terms*—Switched reluctance machine, torque control, current control.**

I. Introduction

INDUSTRIAL interest in Switched Reluctance Motor (SRM) has spurred primarily due to the emerging markets for variable speed drives in consumer and industrial products. The major reasons of these interests for SRM are robustness, high efficiency, low cost (no permanent magnets), high speed, simple structure, fault tolerance [1], easy to maintain, high torque in low speed, simple power converter circuits with reduced number of switches, excellent controllability and smaller dimension of the motor in comparison to the other motors [2]. SRM are now used in various applications requiring high performances such as in electric vehicle propulsion [3]–[8], electromechanical brakes of vehicles [9], automotive starter-generators [10], [11], reluctance generators [12] and aerospace applications [13], [14].

However, the application of SRM in industry is marred by its acoustic noise [15] caused by radial force [16] and excessive torque ripple problem, especially for variable speed applications such as electrical and hybrid vehicules. Torque ripple, efficiency or acoustic noise can be optimized over a wide speed operating range by using electronic control techniques [17]. However such control is complex due to its highly non-linear electromagnetic property of the SRM and power converter propeties. Moreover, the optimization of the torque ripple, efficiency and acoustic noise is not trivial. The optimization of one criterion reduces the performance of the other criteria [18].

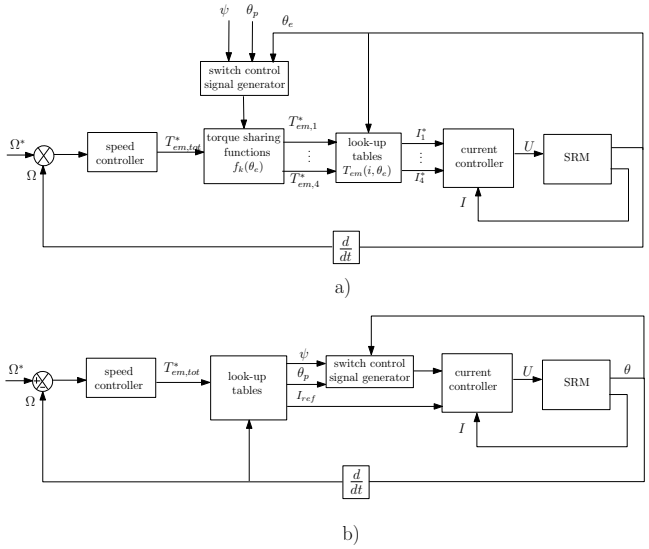

Fig. 1. "Indirect Torque Control" schemes.

Current or torque control techniques constitutes the main control block in drives which obtains the desired high bandwidth in torque and speed responses. Two different methods exist for torque control, i.e., "Indirect Torque Control" and "Direct Torque Control". In former case, the phase current are controlled in order to produce the required torque, while in latter the converter is seen as a hybrid system and phase current are not controlled.

In [19], a method was proposed, which avoids implementation of a high-precision rotor position system and torque commutating current waveforms that strongly depend on the machine parameters, power converter losses, DC-bus voltage, etc. This strategy is called Direct Instantaneous Torque Control (DITC), which is a well-known concept for induction and permanent magnet machine. The important feature of DITC is that the torque is directly controlled by the state of the converter. Therefore, no current control-loop is implemented

978-1-4799-0223-1/13/$31.00 ©2013 IEEE

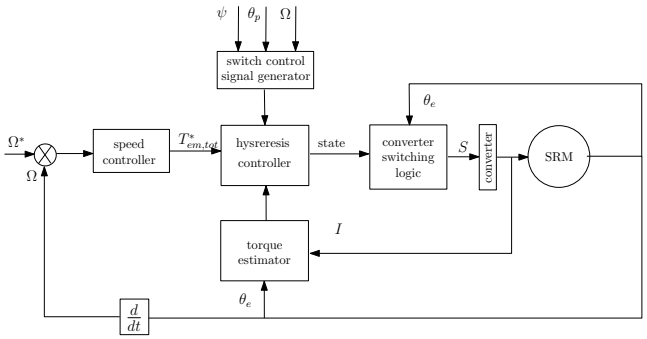

Fig. 2. "Direct Torque Control" scheme.

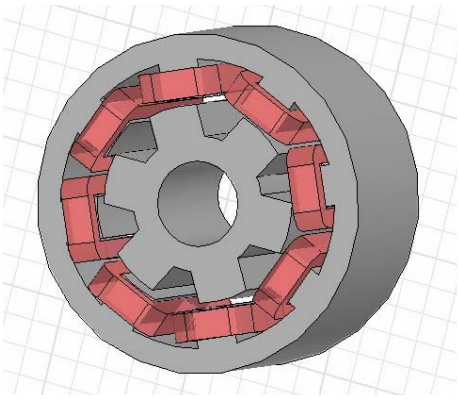

Fig. 3. 3D view of the 8/6 SRM prototype.

and DITC improves torque dynamics compared to the previous strategies [20], [21]. However, industrial electrical systems require the voltage and current to be controlled at the same time due to security reasons. Thus, regular DITC is not preferred in such conditions.

The objective of our work was to extend the regular DITC proposed in [19], [20] such that to control the maximum phase currents.

In section II, an overall layout of DITC of SRM was given; the main drawbacks and advantages are recalled. In section III, an Enhanced Direct Instantaneous Torque Control (EDITC) is presented where additional features such as current limiter was introduced in hysteresis-controller. Section IV validates our controller with simulations done over wide range of speed and torque. Finally, conclusion of our work with some future research on this topic is presented in Section V.

II. Regular DITC

Fig. 2 depicts the overall block diagram of the Direct Instantaneous Torque Control (DITC). DITC constitutes three main blocks: i) A torque estimator based on 2D look-up table, ii) A hyteresis controller, iii) A converter switching logic.

A. Torque estimator

A four phases, $8/6$ SRM prototype as shown in Fig. 3 is considered for our study, where the characteristics of SRM

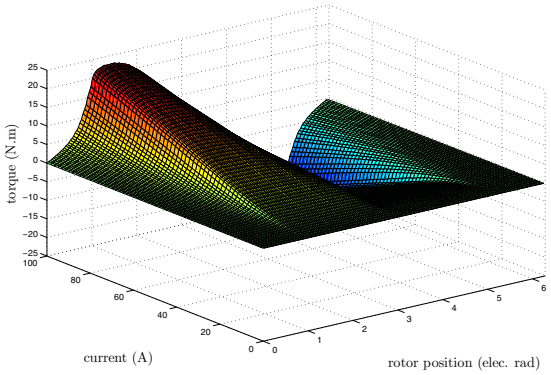

Fig. 4. 3D torque characteristic versus phase current and rotor position.

are listed in table III. The torque estimation is based on the machine magnetization characteristics that are usually obtained from experimental measurements or from numerical calculations such as finite element analysis (FEA). In this study, the flux linkage $\phi(i,\theta)$ and torque $T(i,\theta)$ are generated by a numerical tool called MRVSIM based on FEA [22]. The torque is represented in Fig. 4 over one electrical period and for phase currents going up to 100A. The electromagnetic torque obtained from FEM is stored in look-up table and is feedback to hysteresis controller through linear interpolations. The SRM simulation software [22] does not take into account the mutual inductances. However, it has been shown [23] that the mutual inductance is negligible compared to the self inductance. Thereby here, we assumed that each phases are independent. Moreover, experimental measurement show that the computed torque is in very good accordance with the real produced torque [17].

B. Hysteresis controller

With DITC, the torque is directly controlled by the hysteresis controller; current controller does not exist. Therefore, the 4-phase torques are computed using the 3D-torque characteristic and feedback to the hysteresis controller.

The phases control can be divided into three categories, namely single active phase, double active phase and four active phases (in our case with the continuous conduction mode [17], [24]–[26]). In this paper, we avoided the four active phase and single active phase in order to reduce the torque ripple.

In the double active phase, two phase are excited at the same time. One is defined as primary phase and the other one as secondary phase, as illustrated in Fig 5. For a 4-phase SRM, the electrical position is divided into four parts and according to the position θ and turn on angle ψ, the primary and secondary phases are computed.

The hysteresis controller regulates the torque of one phase by generating the state signals for the half-bridge converter. Only three states are possible, i.e. "1" is active conduction

mode, “0” is for freewheeling mode and “-1” is demagnetization state, as shown on Fig. 6.

To define the state of the primary and secondary converter, a hysteresis controller with four bands is defined [19], [20], as shown on Fig. 7. Commutation process starts when an incoming phase is activated, i.e. at t_{on}. The outgoing phase changes from active to freewheeling state. Just then the total torque drops below the outer hysteresis band, i.e. $T < T^* - \Delta H$, the outgoing phase is magnetized again. Hence the total torque increases and is regulated within outer hysteresis band. When the incoming phase is able to build up total torque the outgoing phase is again switched to freewheeling state, i.e. for $T > T^* - \delta h$. When the total torque rises above the outer hysteresis $T > T^* + \Delta H$, the outgoing phase is demagnetized in order to reduce the total torque. By the end of conduction period, i.e at t_{off}, the outgoing phase is totally demagnetized. This DITC regulates the torque instantaneously and is independent of position and switching angles. Furthermore, the switching strategy performs phase commutation automatically. A detailed analysis can be found in [19], [20].

Fig. 8 shows the normal switching logic of hysteresis controller where the converter switching states are shown in Tab. I. The transition of state 0 to state 1 is only during start operation and for all other operation state 0 is considered emergency braking.

C. Advantages and drawbacks of DITC

In-spite having better torque dynamics, as stated before, DITC have two main issues: over commutation of the converters (see Fig. 7) when the total torque is outside $T^* \pm \Delta H$ and no current control. Therefore in order to improve the regular DITC, extension of current DITC was conducted in this paper,

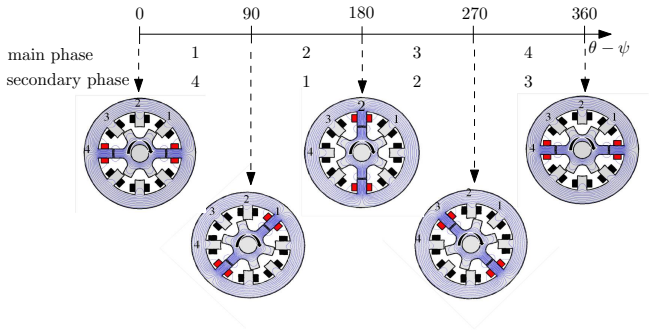

Fig. 5. Switching logic.

TABLE I
SWITCHES STATE CONVERTER ACCORDING THE STATE.

State	Incoming phase	Outgoing phase
0 Emergency stop	-1	-1
1	0	0
2	1	0
3	1	1

main phase \ secondary phase	1	0	-1
1	(1,1)		
0	(1,0)	(0,0)	
-1		(0,-1)	

Fig. 6. Switching state of the converter.

namely: i) Over or under torque control, ii) Current limitation while controlling the desired torque.

III. Enhanced DITC

A. Over or under torque production

During commutation, when the total torque rises above the outer hysteresis band $T > T^* + \Delta H$, the outgoing phase is demagnetized instead. However, the phenomenon could be repeated many time as illustrated in Fig. 7. As the duration of demagnetization of the outgoing phase was too short, it led to an over or under torque production. Hence we proposed a flag that is used to keep a check on increase in torque when both phases are magnetized. If $N_1 > N_{1max}$ (see Fig. 9, N_{1max} as to be define by the user) then demagnetization phase is kept until the total torque is lower than $T < T^* - \delta h$. Similarly N_2 flag is used to keep check on decrease in torque when incoming phase is freewheeling and outgoing phase is demagnetized. If $N_2 > N_{2max}$ then immediately incoming phase is magnetized and outgoing phase goes to freewheeling mode so as to increase the torque of SRM.

B. Current limiter

Current limiter was introduced in hysteresis controller so as to keep check on maximum current in each phase. When the current of incoming phase and outgoing phase are within limits, then the operation of hysteresis controller is same as in Fig. 9. However, when the currents exceed the maximum limit, new states are added in order to limit the current without compromising the torque performance, as shown in Fig. 10.

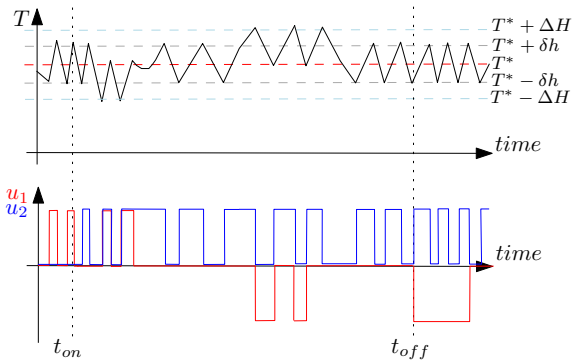

Fig. 7. Torque and voltages waveforms example for phase 1 and 2.

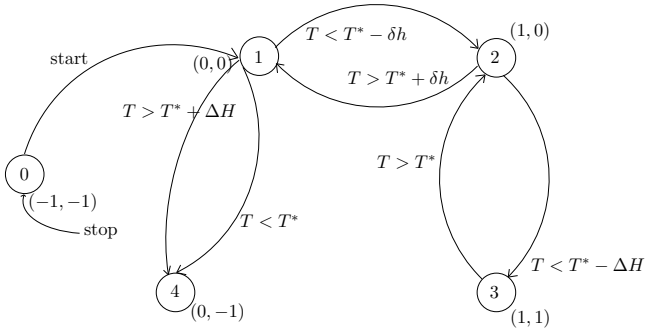

Fig. 8. State machine of the regular DITC.

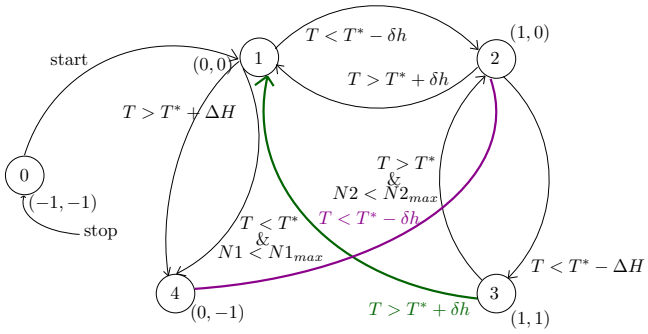

Fig. 9. Enhanced state machine of the regular DITC with flag.

As shown in table II, when the active state is 1 and $T < T^* - \delta h$, the state 2 will go to active mode. However, because the main current I_p has reached the current limit I_{max}, state 2 is forbidden. In order to respect the desired torque, a new state 5 is added. Here, the incoming phase is demagnetized in order to reduce the current I_p and the outgoing phase is magnetized in order to maintain the torque.

In the same manner, if the active state is 3, the only solution in order to reduce the incoming phase current is by introducing state 6. However in this case the current is limited but the desired torque is not maintained. Finally, if at next step the incoming phase current is lower than the maximum value, then the state 5, 6 and 7 are switched to state 1 or 2 (regular state machine).

TABLE II
SWITCHES STATE CONVERTER FOR THE EDITC.

State	Incoming phase	Outgoing phase
0 Emergency stop	-1	-1
1	0	0
2	1	0
3	1	1
4	0	-1
5	-1	1
6	0	1
7	1	-1
8	-1	0

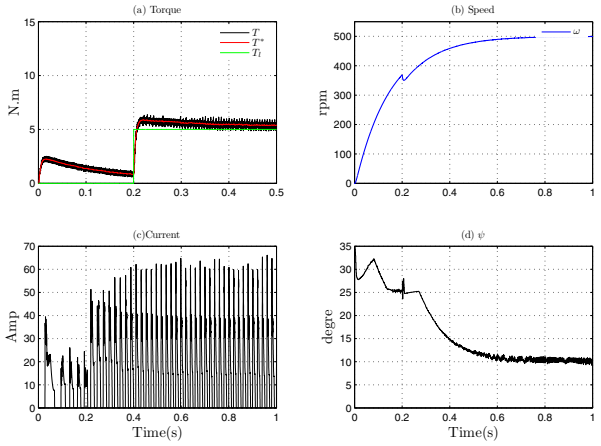

Fig. 11. Simulated torque (5 N.m), speed (500 rpm) and current waveform for the EDTIC.

IV. Simulation Results

Simulations were performed for a four phase, 8/6 SRM prototype (Table 3). It is shown that the performance of EDITC enables smooth torque up to nominal speed and nominal torque.

Figs. 11, 12 and 13 shows the simulation of the EDITC of SRM for different speed and torque. Figs. 11(a), 12(a) and 13(a) shows the instantaneous torque and reference torque of SRM while Figs. 11(b), 12(b) and 13(b) is the speed achieved by SRM. Figs. 11(c), 12(c) and 13(c) is the current of one phase of SRM, while Figs. 11(d), 12(d) and 13(d) is graph of angle ψ.

Fig. 14 shows the performance of DITC for various speed and torque without current limiter. It can be seen than the current rises above the maximum limit (here fix at 100A) of current.

A comparative simulation with current limiter is shown in Fig. 15. It can be noted that the current limiter is effective in limiting the current of SRM without any loss of performance.

V. Conclusion

A modified Direct Torque Control for SRM was proposed in this paper. The main issue of regular DITC is that the current is measured but not controlled. Therefore, an Enhanced DITC algorithm was provided which included additional feature such as current limiter without compromising the desired torque level. Several simulations are presented which validates our controller over wide range of speed and torque.

When hysteresis band is kept constant, the switching frequency grows rapidly as torque level decreases. High switching frequency increases switching loses. The future work should ponder into adopting the torque control while maintaining switching frequency constant and outside the mechanical vibration of the machine.

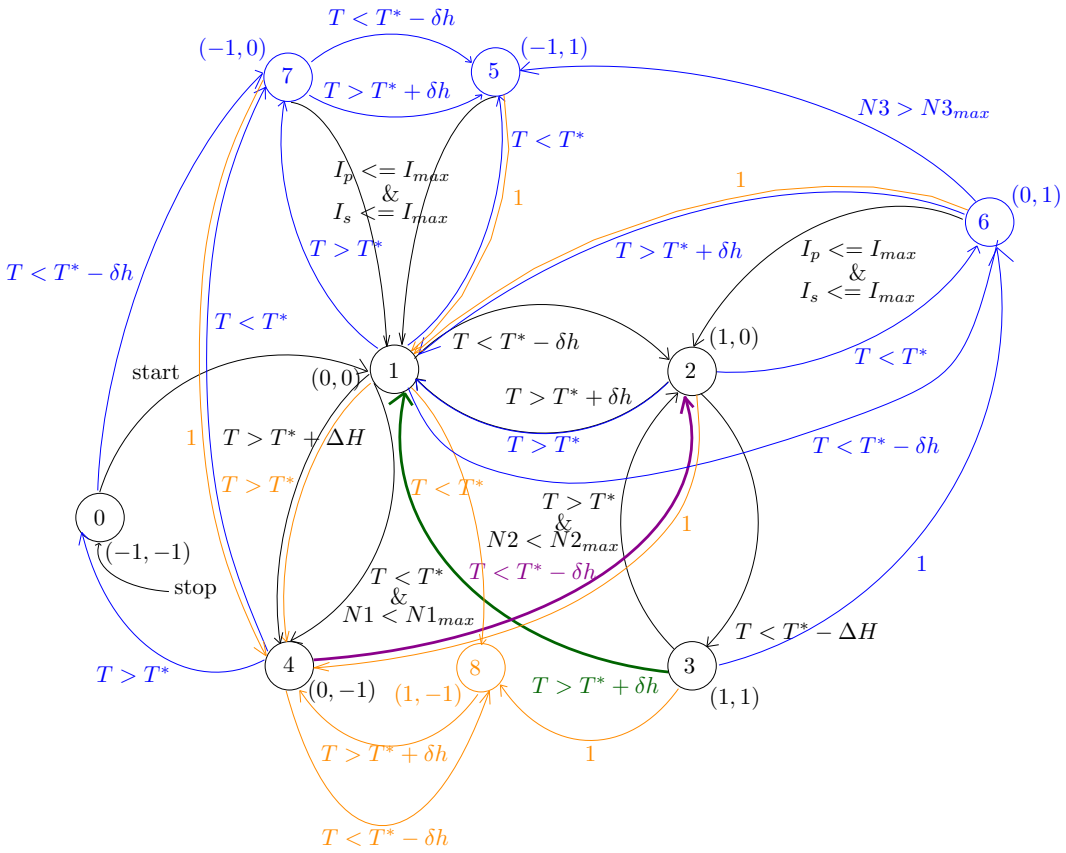

Fig. 10. Enhanced state machine of the regular DITC with flag and current control.

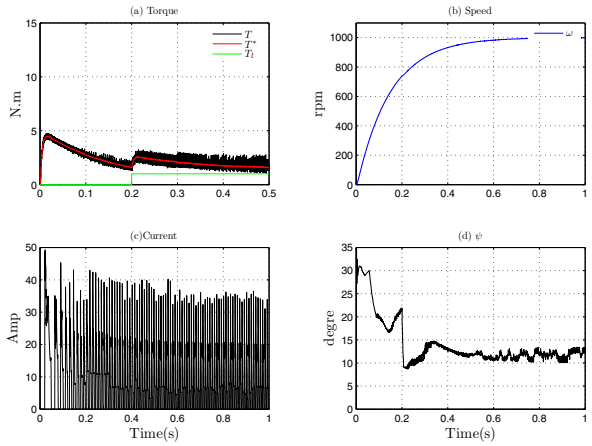

Fig. 12. Simulated torque (2 N.m), speed (1000 rpm) and current waveform for the EDTIC.

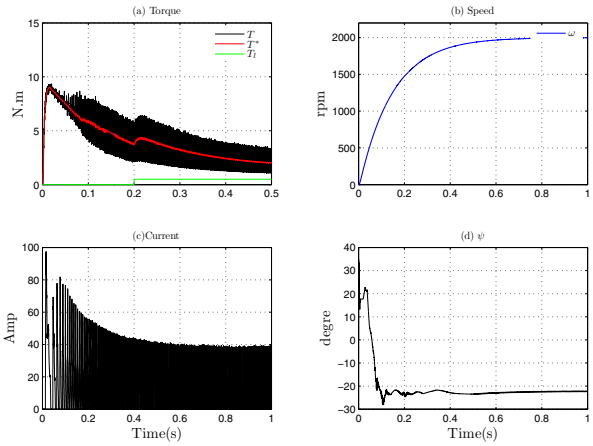

Fig. 13. Simulated torque (1 N.m), speed (2000 rpm) and current waveform for the EDTIC.

REFERENCES

[1] L. Szabo and M. Ruba, "Segmental stator switched reluctance machine for safety-critical applications," *IEEE Transactions on Industry Applications*, vol. 48, no. 6, pp. 2223–2229, 2012.

[2] T. Bass, M. Ehsani, T. Miller, and R. Steigerwald, "Development of a unipolar converter for variable reluctance motor drives," *IEEE Transactions on Industry Applications*, vol. IA-23, pp. 545–553, 1987.

[3] B. Kalan, H. Lovatt, and G. Prout, "Voltage control of switched reluctance machines for hybrid electric vehicles," *IEEE Power Electronics Specialists Conference (PESC'02)*, vol. 4, pp. 1656–1660, 2002.

[4] H. Lim, R. Krishnan, and N. Lobo, "Design and control of a linear propulsion system for an elevator using linear switched reluctance motor drives," *IEEE Transactions on Industrial Electronics*, vol. 55, no. 2, pp. 534–542, 2008.

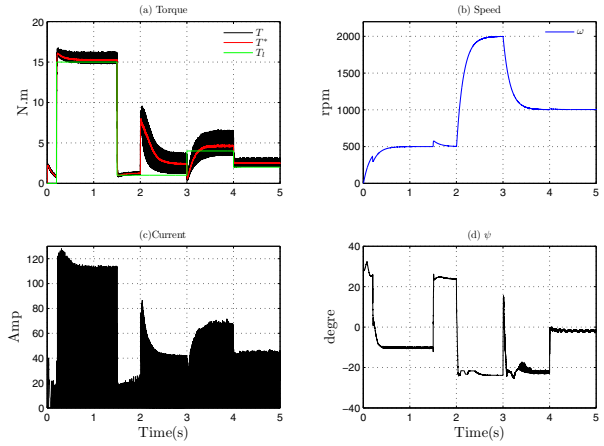

Fig. 14. Simulated torque, speed and current waveform with no current limiter for the DTIC.

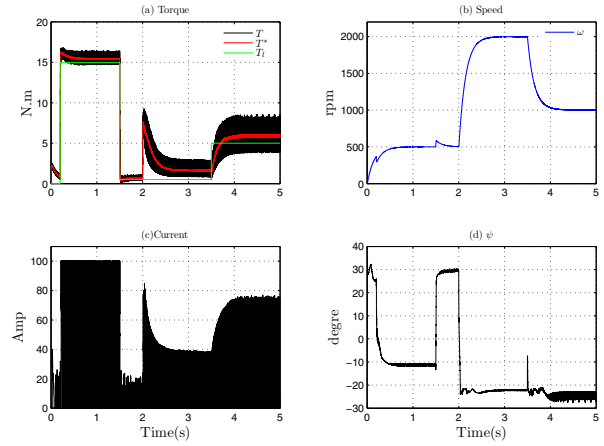

Fig. 15. Simulated torque, speed and current waveform with current limiter for the EDTIC.

[5] H. Chang and C. Liaw, "Development of a compact switched-reluctance motor drive for ev propulsion with voltage boosting and pfc charging capabilities," *IEEE Transactions on Vehicular Technology*, vol. 58, no. 7, pp. 3198–3215, Sept. 2009.

[6] M. Takeno, A. Chiba, N. Hoshi, S. Ogasawara, M. Takemoto, and M. Rahman, "Test results and torque improvement of the 50-kw switched reluctance motor designed for hybrid electric vehicles," *IEEE Transactions on Industry Applications*, vol. 48, no. 4, pp. 1327–1334, 2012.

[7] B. Bilgin, A. Emadi, and M. Krishnamurthy, "Comprehensive evaluation of the dynamic performance of a 6/10 srm for traction application in phevs," *IEEE Transactions on Industrial Electronics*, vol. PP, no. 99, 2013.

[8] K. Kiyota, "Design of switched reluctance motor competitive to 60 kw ipmsm in third generation hybrid electric vehicle," *IEEE Transactions on Industry Applications*, vol. PP, no. 99, 2013.

[9] P. Krishnamurthy, W. Lu, F. Khorrami, and A. Keyhani, "Robust force control of an srm-based electromechanical brake and experimental results," *IEEE Transactions on Control Systems Technology*, vol. 17, no. 6, pp. 1306–1317, Nov. 2009.

[10] B. Fahimi, A. Emadi, and R. Sepe, "A switched reluctance machinebased starter/alternator for more electric cars," *IEEE Industry Applications Magazine*, vol. 20, no. 1, pp. 116–124, Mar. 2004.

[11] J. Faiz and K. Moayed-Zadeh, "Design of switched reluctance machine for starter/generator of hybrid electric vehicle," *Electric Power Systems Research, Elsevier*, vol. 75, no. 2-3, pp. 153–160, 2005.

[12] S. Narla, "Switched reluctance generator controls for optimal power generation and battery charging," *IEEE Transactions on Industry Applications*, vol. 48, no. 5, pp. 1452–1459, Sept.-Oct. 2012.

[13] A. Radun, "High-power density switched reluctance motor drive for aerospace applications," *IEEE Transactions on Industry Applications*, vol. 28, no. 1, pp. 113–119, 1992.

[14] R. Naayagi and V. Kamaraj, "Shape optimization of switched reluctance machine for aerospace applications," *Proceedings of the 31st Annual Conference of IEEE Industrial Electronics Society (IECON'05)*, Nov. 2005.

[15] K. Kasper, J. Fiedler, D. Schmitz, and R. D. Doncker, "Noise reduction control strategies for switched reluctance drives," in *IEEE Vehicle Power and Propulsion Conference (VPPC'06)*, 2006.

[16] J. Fiedler, K. Kasper, and R. D. Doncker, "Calculation of the acoustic noise spectrum of srm using modal superposition," *IEEE Transactions on Industrial Electronics*, vol. 57, no. 9, pp. 2939–2945, Sep. 2010.

[17] H. Hannoun, M. Hilairet, and C. Marchand, "Design of an srm speed control strategy for a wide range of operating speeds," *IEEE Transactions on Industrial Electronics*, vol. 57, no. 6, pp. 2911–2921, Sept. 2010.

[18] A. Kolli, G. Krebs, X. Mininger, and C. Marchand, "Impact of command parameters on efficiency, torque ripple and vibrations for switched reluctance motor," in *XXth International Conference on Electrical Machines (ICEM 2012)*, Sept. 2012.

[19] R. Inderka and R. W. Doncker, "Ditc-direct instantaneous torque control of switched reluctance drives," *37th Annual Meeting of the IEEE Industrial Application Society (IEEE-IAS)*, 2002.

[20] N. Fuengwarodsakul, M. Menne, R. Inderka, and R. D. Doncker, "High-dynamic four-quadrant switched reluctance drive based on ditc," *IEEE Transactions on Industry Applications*, vol. 41, no. 5, pp. 1232– –1242, Sep./Oct. 2005.

[21] H. Brauer, M. Hennen, and R. D. Doncker, "Control for polyphase switched reluctance machines to minimize torque ripple and decrease ohmic machine losses," *IEEE Transactions on Power Electronics*, vol. 27, no. 1, pp. 370–378, 2012.

[22] M. Besbes and B. Multon, "Mrvsim logiciel de simulation et d'aide à la conception de machines à réluctance variable à double saillance à alimentation électronique," French Patent Deposit APP CNRS n.IDDN.FR.001.430 010.000.S.C.2004.000.30 645., 2004.

[23] Y. Sofiane, A. Tounzi, and F. Piriou, "A non linear analytical model of switched reluctance machines," *The European Physical Journal - Applied Physics*, pp. 163–172, 2002.

[24] M. Rekik, M. Besbes, C. Marchand, B. Multon, S. Loudot, and D. Lhotellier, "High-speed-range enhancement of switched reluctance motor with continuous mode for automotive applications," *European Transactions on Electrical Power*, vol. 18, pp. 674–693, 2008.

[25] N. Schofield, S. Long, D. Howe, and M. McClelland, "Design of a switched reluctance machine for extended speed operation," *IEEE Transactions on Industry Applications*, vol. 45, no. 1, pp. 116–122, Jan-Feb 2009.

[26] H. Hannoun, M. Hilairet, and C. Marchand, "Experimental validation of a switched reluctance machine operating in continuous-conduction mode," *IEEE Transactions on Vehicular Technology*, vol. 60, no. 4, pp. 1453–1460, May 2011.

TABLE III
PROTOTYPE CHARACTERISTICS

Geometric parameters			
Number of rotor poles	6	Stator pole arc	19.8^0
Number of stator poles	8	Rotor pole arc	20.65^0
Stator outer diameter	143 mm	Airgap lebgth	0.8 mm
Shaft diameter	23 mm		
Electrical parameters			
Number of phases	4	Nominal speed	3000 rpm
Nominal power	1.2 kW	Nominal voltage	24 V